Available online at www.sciencedirect.com
SCIENCE DIRECT®
Journal of Sound and Vibration 274 (2004) 13–37
JOURNAL OF SOUND AND VIBRATION
www.elsevier.com/locate/jsvi

Dynamic response analysis of a liquid-filled cylindrical tank with annular baffle

K.C. Biswal[a,1], S.K. Bhattacharyya[b], P.K. Sinha[a,*]

[a] *AR & DB Centre of Excellence for Composite Structures Technology, Department of Aerospace Engineering, Indian Institute of Technology, Kharagpur 721302, India*
[b] *Department of Civil Engineering, Indian Institute of Technology, Kharagpur 721302, India*

Received 29 October 2002; accepted 19 May 2003

Abstract

Baffles are generally used as damping devices in liquid storage tanks. The focus of the present paper is to study the influence of a baffle on the dynamic response of a partially liquid-filled cylindrical tank. A baffle is assumed here to have the shape of a thin annular circular plate. The natural frequencies of an inviscid and incompressible liquid are determined for varying positions and dimensions of a baffle attached normal to the tank wall. The flexibility of both the baffle and the tank are considered in studying the effects of liquid–baffle and liquid–tank interactions on the sloshing mode frequencies. Finite element codes are developed and are then used to analyze both the liquid domain and the structural domain (i.e., the tank and the baffle). The coupled vibration frequencies of the tank–baffle system are computed considering the effect of sloshing of liquid. The results obtained for a liquid-filled elastic tank without a baffle and a rigid tank with a rigid baffle are in good agreement with the available results. The slosh amplitude of liquid in a rigid tank with and without a rigid baffle is studied under translational base excitation. The effects of the tank wall and baffle flexibility on the slosh response are also investigated.

1. Introduction

Sloshing is the motion of liquid in a container with a free surface. The coupled interaction between the sloshing liquid and the structure has been the challenging field of research in many engineering applications such as liquid storage tanks, fuel tanks of space vehicles, dam–reservoir systems and several others.

*Corresponding author. Tel.: +91-3222-283016; fax: +91-3222-2553003.
E-mail address: pksinha@aero.iitkgp.ernet.in (P.K. Sinha).
[1] On study leave from REC, Rourkela 769008, India.

0022-460X/03/$ - see front matter © 2003 Elsevier Ltd. All rights reserved.
doi:10.1016/S0022-460X(03)00568-6

Housner [1] presented the simplified formulae to compute the dynamic pressures developed on accelerated liquid containers. Housner [2] studied the dynamic behaviour of ground-supported elevated water tanks considering equivalent spring–mass systems. The dynamic behaviour of liquid in moving containers was presented by Abramson [3] in the form of a monograph NASA SP-106. Zienkiewicz and Bettess [4] addressed Lagrangian and Eulerian approaches for the solution of coupled structure and fluid systems. Haroun and Housner [5] used analytical and finite element models for liquid and tank, respectively, for the dynamic analysis of ground-supported cylindrical tanks. Aslam [6] developed a finite element formulation based on a linearized wave theory to predict the slosh displacements and hydrodynamic pressure in an axisymmetric rigid tank due to an arbitrary ground acceleration. Aslam et al. [7] studied the sloshing response of liquid in annular and cylindrical tanks both analytically and experimentally. Li et al. [8] analyzed the liquid sloshing response in a pool due to three-directional earthquake ground motions. The coupling effect between the sloshing liquid and the flexible fluid-filled system was studied by Balendra et al. [9]. Ma et al. [10] evaluated the seismic response of shell structures containing a fluid with the aid of the added-mass concept. Liu and Ma [11] developed a coupled fluid–structure finite element method for the seismic analysis of fluid-filled system of various geometries. Olson and Bathe [12] used the displacement-based fluid finite elements for calculating the fluid–structure frequencies. A new Lagrangian fluid method was developed by Wilson and Khalvati [13] which selectively eliminates the zero-energy modes and produces a fluid element with optimum behaviour. The method involves the introduction of the constraint of zero fluid rotation at the integration points. Gupta and Hutchinson [14] carried out studies on ground-supported cylindrical storage tanks vibrating in an axisymmetric manner. Lui [15] studied the dynamic coupling of a liquid–tank system under transient excitations. The closed-form solutions for the element stiffness and mass matrices for the axisymmetric thin shell was obtained by To and Wang [16]. Kock and Olson [17] developed a finite element method for analyzing non-linear and linear fluid–structure interaction problems by working directly from a variational indicator based on Hamilton's principle. The free vibration characteristics of anisotropic thin cylinder, partially or completely filled with liquid was studied by Lakis and Sinno [18] using a new method which combines classical thin shell theory with finite element analysis. A finite element method with a reduction technique had been used by Qinque and Lidu [19] for solving the eigenproblem associated with the liquid–container coupling. The coupled frequencies of a liquid in a cylindrical container with an elastic liquid surface cover had been determined analytically by Bauer [20]. The natural frequencies of annular plates on an aperture of an infinite rigid wall and in contact with a fluid on one side are theoretically obtained by Amabili et al. [21] using the added-mass approach. The authors applied Hankel transform to solve the fluid–plate coupled system and expressed the boundary conditions by integral equations. Babu and Bhattacharyya [22] developed the finite element model for the fluid and structure domains and solved the coupled fluid–tank problem using Newmark predictor–multi-corrector algorithm. Goncalves and Ramos [23] presented an effective modal solution for evaluating the free characteristics of cylindrical shells, partially or completely filled with liquid. Kim et al. [24] used Rayleigh–Ritz method to evaluate the dynamic response of rectangular flexible fluid containers under horizontal and vertical ground excitation. Bermudez et al. [25] carried out a finite element analysis for the solution of incompressible fluid–structure vibration problems.

Amabili et al. [26] studied the dynamic characteristics of partially filled cylindrical tanks with a flexible bottom and ring stiffeners. Cho and Song [28] presented two separate dynamic models, the rigid-tank sloshing and the bulging model without liquid free-surface sloshing, for an eigenanalysis of fluid–structure interaction problems.

Most of the published works are concerned with the slosh frequency and response analysis of liquid-filled tanks without baffle. Gedikli and Ergüven [27] employed boundary element method to study the effects of baffle on the natural frequencies and seismic response of liquid in a circular cylindrical tank. However, both tank and baffle are considered as rigid. The natural frequencies of liquid in a rigid tank with flexible baffles had recently been studied by Biswal et al. [29]. The analysis considered only the asymmetric mode of vibration of liquid and flexible baffle corresponding to the circumferential wave number as one.

A coupled liquid–structure finite element method is developed in this paper for computing the sloshing mode frequencies of liquid and coupled vibration mode frequencies of the liquid–structure system. The present formulation considers all circumferential modes. The flexibility of both tank and baffle is taken into account. The slosh amplitude of liquid in a partially filled tank with baffle are computed under translational base acceleration taking the liquid–baffle and the liquid–tank interaction into account.

2. Governing equations and finite element formulation

A liquid-filled cylindrical tank with a baffle is shown in Fig. 1. The base of the tank is assumed to be rigid. The liquid in the tank is assumed to be incompressible, inviscid and irrotational. The governing differential equation for the liquid in terms of pressure variable is

$$\nabla^2 P = 0 \tag{1}$$

in which $P = P(r, \theta, z, t)$ is the liquid dynamic pressure and

$$\nabla^2 = \frac{\partial^2}{\partial r^2} + \frac{1}{r}\frac{\partial}{\partial r} + \frac{1}{r^2}\frac{\partial^2}{\partial \theta^2} + \frac{\partial^2}{\partial z^2}.$$

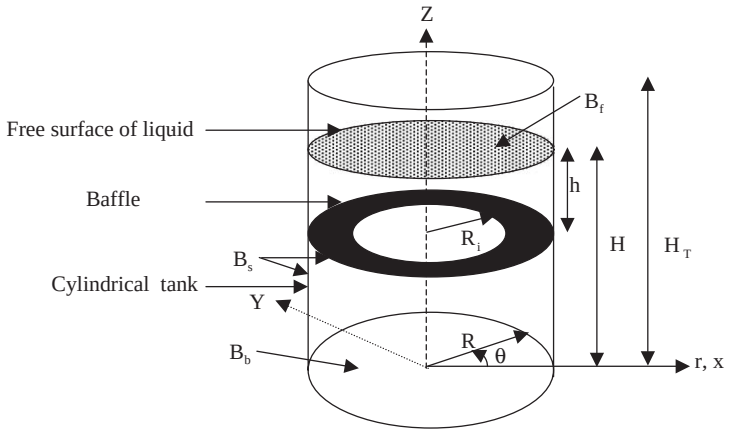

Fig. 1. A cylindrical tank with a baffle.

Eq. (1) is solved using finite element technique and with the appropriate time-dependent boundary conditions as specified below:

(a) *At liquid–structure interface*:

$$\partial P/\partial n = -\rho_f \ddot{d}_n \quad \text{on } B_s, \tag{2}$$

where ρ_f is the density of the liquid; d_n is the displacement of the structure; n is the outwardly drawn normal to the surface of the structure.

(b) *At liquid free surface*:

The linearized free-surface condition yields

$$\partial^2 P/\partial t^2 + g\partial P/\partial n = 0 \quad \text{on } B_f. \tag{3}$$

However, if free-surface wave of the liquid is ignored, then $P = 0$.

(c) *At the bottom of the tank*:

$$\partial P/\partial n = 0 \quad \text{on } B_b. \tag{4}$$

2.1. Idealization of tank

The cylindrical tank, the geometry of which is that of a shell-of-revolution having a constant radius R and thickness t_t, with the wall connected to rigid base is shown in Fig. 1. The axial, circumferential and radial displacement components of a point on the tank middle surface are u, v and w, respectively.

The tank material is assumed to be homogeneous, isotropic and linearly elastic. The force and moment resultants can be expressed in terms of the midsurface strains, ε^0_{zz}, $\varepsilon^0_{\theta\theta}$, $\varepsilon^\theta_{z\theta}$ and curvatures χ_{zz}, $\chi_{\theta\theta}$, $\chi_{z\theta}$ as defined below:

$$\{\sigma\} = [D]\{\varepsilon\} \tag{5}$$

in which

$$\{\sigma\}^{\mathrm{T}} = [\,N_{zz} \quad N_{\theta\theta} \quad N_{z\theta} \quad M_{zz} \quad M_{\theta\theta} \quad M_{z\theta}\,];$$
$$\{\varepsilon\}^{\mathrm{T}} = [\,\varepsilon^0_{zz} \quad \varepsilon^0_{\theta\theta} \quad \varepsilon^0_{z\theta} \quad \chi_{zz} \quad \chi_{\theta\theta} \quad \chi_{z\theta}\,].$$

The kinematic relations are based on the bending of thin shell [30]:

$$\{\varepsilon\} = \{\varepsilon^0\} + \bar{r}\{\chi\}. \tag{6}$$

2.2. Finite element formulation

The cylindrical tank is modelled by two-noded ring elements with four degrees of freedom (three displacements u, v, w and one rotation) per node. Fig. 2 shows two axisymmetric thin shell elements with a baffle element with node j as common node.

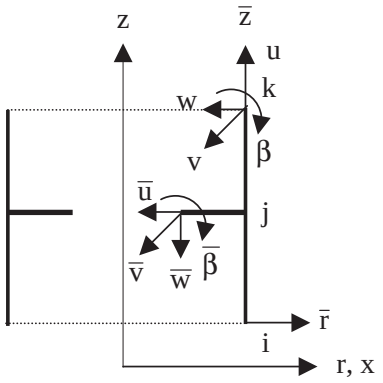

Fig. 2. Two tank elements and a baffle element.

The axial, circumferential and radial components of displacement of a point on the middle surface of the shell may be expressed as

$$u = \sum_{i=1}^{2} S_i u_i \cos n\theta, \tag{7}$$

$$v = \sum_{i=1}^{2} S_i v_i \sin n\theta, \tag{8}$$

$$w = \left[\sum_{i=1}^{2} N_i w_i + \sum_{i=1}^{2} \hat{N}_i \beta_i\right] \cos n\theta, \tag{9}$$

where

$$S_1 = 1 - p, \quad S_2 = p;$$
$$N_1 = (1 - 3p^2 + 2p^3), \quad N_2 = (3p^2 - 2p^3);$$
$$\hat{N}_1 = L(p - 2p^2 + p^3), \quad \hat{N}_2 = L(-p^2 + p^3);$$
$$p = z/L;$$

n is the circumferential wave number.

The element stiffness matrix is written as

$$[K_t]^e = \pi R \int_0^L [B]^{\mathrm{T}}[D][B]\,\mathrm{d}z, \tag{10}$$

where $[B]$ and $[D]$ are given in Ref. [22].

The mass matrix is given by

$$[M_t]^e = \pi \rho t R \int_0^L [N]^{\mathrm{T}}[N]\,\mathrm{d}z, \tag{11}$$

where

$$[N] = \begin{bmatrix} S_1 & 0 & 0 & 0 & S_2 & 0 & 0 & 0 \\ 0 & S_1 & 0 & 0 & 0 & S_2 & 0 & 0 \\ 0 & 0 & N_1 & \hat{N}_1 & 0 & 0 & N_2 & \hat{N}_2 \end{bmatrix}.$$

2.3. Idealization of baffle

An annular thin circular plate is used as a baffle. The assumed displacement functions are expressed in polar co-ordinates (r and θ):

$$\bar{u} = (\alpha_1 + \alpha_2 r)\cos n\theta, \tag{12}$$

$$\bar{v} = (\alpha_3 + \alpha_4 r)\sin n\theta, \tag{13}$$

$$\bar{w} = (\alpha_5 + \alpha_6 r + \alpha_7 r^2 + \alpha_8 r^3)\cos n\theta \tag{14}$$

and the nodal displacements for each element are

$$\{\bar{d}\} = \{\bar{u}_1 \quad \bar{v}_1 \quad \bar{w}_1 \quad \bar{\beta}_1 \quad \bar{u}_2 \quad \bar{v}_2 \quad \bar{w}_2 \quad \bar{\beta}_2\}, \tag{15}$$

where $\bar{u}$, $\bar{v}$ and $\bar{w}$ are axial, circumferential and transverse displacements, respectively, and $\bar{\beta}$, the rotation.

The strain–displacement relationships for axisymmetric shell geometry are given in Ref. [30]. These relations are used to derive the matrix $[\bar{B}]$ for flat baffle geometry.

The element stiffness matrix is given by

$$[\bar{K}_b]^e = \int_0^{2\pi} \int_{R_1}^{R_2} [\bar{B}]^{\mathrm{T}}[\bar{D}][\bar{B}] r \, \mathrm{d}r \, \mathrm{d}\theta, \tag{16}$$

where R_1 and R_2 are inner and outer radii, respectively, for the annular ring elements and r varies from R_1 to R_2. The $[\bar{D}]$ matrix is obtained in similar way as that of tank.

The element mass matrix is expressed as

$$[\bar{M}_b]^e = \pi\rho t \int_{R_1}^{R_2} [\bar{N}]^{\mathrm{T}}[\bar{N}] r \, \mathrm{d}r, \tag{17}$$

where

$$[\bar{N}] = \begin{bmatrix} 1 & r & 0 & 0 & 0 & 0 & 0 & 0 \\ 0 & 0 & 1 & r & 0 & 0 & 0 & 0 \\ 0 & 0 & 0 & 0 & 1 & r & r^2 & r^3 \end{bmatrix}.$$

2.4. Tank–baffle system

The tank co-ordinate system is taken as the global co-ordinates for the structure domain. The element stiffness and mass matrices of baffle are appropriately transformed according to the

global co-ordinate system. The element stiffness and mass matrices of tank and baffle are assembled to obtain the global stiffness and mass matrices of tank–baffle system.

2.5. Idealization of liquid

The finite element formulation is based on Galerkin weighted residual method. A four-noded isoparametric quadrilateral axisymmetric element is used to discretize the liquid domain. The liquid dynamic pressure ($\bar{P}$) is approximated as

$$\bar{P}(r,\theta,z,t) = \sum_{j=1}^{N} N_j P_j(t), \tag{18}$$

where $N_j = \bar{N}_j(r,z)\cos n\theta$; $\bar{N}_j$ are the shape functions in two dimensions and $P_j(t)$ are the time-dependent nodal pressures.

The finite element form of the governing equation may be written as

$$\int_V \left(\frac{\partial N_i}{\partial r} \sum_1^N \frac{\partial N_j}{\partial r} P_j + \frac{1}{r^2} \frac{\partial N_i}{\partial \theta} \sum_1^N \frac{\partial N_j}{\partial \theta} P_j + \frac{\partial N_i}{\partial z} \sum_1^N \frac{\partial N_j}{\partial z} P_j \right) \mathrm{d}V + \frac{1}{g} \int_{B_f} N_i \sum_1^N N_j \ddot{P}_j \, \mathrm{d}s = - \int_{B_s} \rho_f N_i \ddot{d}_n \, \mathrm{d}s \tag{19}$$

or in standard notations

$$[M_f]\{\ddot{P}\} + [K_f]\{P\} = \{F_p\} \tag{20}$$

in which $[M_f]$, $[K_f]$ and $\{F_p\}$ are liquid mass matrix, liquid stiffness matrix and liquid force vector, respectively.

Eq. (20) may be rewritten as

$$[M_f]\{\ddot{P}\} + [K_f]\{P\} = -\rho_f [S]\{\ddot{d}\} + \{F_{el}\} \tag{21}$$

where

$$[S] = \int_{B_s} [N_f]^{\mathrm{T}} [N_s] \, \mathrm{d}s,$$

with $[N_f]$ as the shape function for the liquid element, $[N_s]$ as the shape function for the structural elements and $\{F_{el}\}$ as the external nodal force.

The free vibration equation may be written as

$$[M_f]\{\ddot{P}\} + [K_f]\{P\} = -\rho_f [S]\{\ddot{d}\}. \tag{22}$$

The equations of motions of tank–baffle system when subjected to external forces and forces due to liquid dynamic pressure takes the following form:

$$[M_s]\{\ddot{d}\} + [K_s]\{d\} = \{F_{et}\} + \{F_l\}, \tag{23}$$

where $[M_s]$ and $[K_s]$ are the mass and stiffness matrices of the tank–baffle system; $\{\ddot{d}\}$ and $\{d\}$ are the generalized nodal accelerations and displacements, respectively. $\{F_{et}\}$ is the external nodal forces. $\{F_l\}$ is the nodal forces exerted on the tank–baffle system due to liquid dynamic pressure and equal to $[S]^{\mathrm{T}}\{P\}$.

Eq. (23) may be written as

$$[M_s]\{\ddot{d}\} + [K_s]\{d\} = \{F_{et}\} + [S]^{\mathrm{T}}\{P\}. \tag{24}$$

Eqs. (21) and (24) are coupled, second order, ordinary differential equations which define the coupled liquid–tank–baffle system completely. These sets of coupled equations are solved using Newmark's predictor–multi-corrector algorithm. The liquid–structure interaction is studied by transferring the tank and baffle normal acceleration to the liquid domain and liquid pressure to the tank–baffle system at the liquid–structure interface. The displacements of the two fields are calculated in a iterative manner within each time step till the desired level of convergence is achieved.

In the absence of external forces, Eq. (24) may be expressed as

$$[M_s]\{\ddot{d}\} + [K_s]\{d\} = [S]^{\mathrm{T}}\{P\}. \tag{25}$$

Eqs. (22) and (25) may be written in matrix form as

$$\begin{bmatrix} [M_s] & [0] \\ \rho_f[S] & [M_f] \end{bmatrix} \begin{Bmatrix} \ddot{d} \\ \ddot{p} \end{Bmatrix} + \begin{bmatrix} [K_s] & -[S]^{\mathrm{T}} \\ [0] & [K_f] \end{bmatrix} \begin{Bmatrix} d \\ p \end{Bmatrix} = \begin{Bmatrix} 0 \\ 0 \end{Bmatrix}. \tag{26}$$

Eq. (26) is rearranged in order to obtain the symmetric matrices for the coupled system, as given by

$$\begin{bmatrix} [K_s] & [0] \\ [0] & [M_f] \end{bmatrix} \begin{Bmatrix} \ddot{d} \\ \ddot{P} \end{Bmatrix} + \begin{bmatrix} [K_s][M_s]^{-1}[K_s] & -[K_s][M_s]^{-1}[S]^{\mathrm{T}} \\ -\rho_f[S][M_s]^{-1}[K_s] & [K_f] + \rho_f[S][M_s]^{-1}[S]^{\mathrm{T}} \end{bmatrix} \begin{Bmatrix} d \\ P \end{Bmatrix} = \begin{Bmatrix} 0 \\ 0 \end{Bmatrix}. \tag{27}$$

Denoting ω_k as the kth natural frequency of the coupled system and $\{\varphi_k\}$ the corresponding mode shape vector, Eq. (27) becomes

$$[\hat{K}]\{\varphi_k\} - \omega_k^2[\hat{M}]\{\varphi_k\} = \{0\}. \tag{28}$$

2.5.1. Sinusoidal base excitation

If the tank is excited under sinusoidal horizontal base excitation, $\ddot{x} = -x_0\omega^2 \sin \omega t$, where x_0 and ω are the amplitude and circular frequency, respectively, it will excite only antisymmetric modes that correspond to circumferential wave number as one. The acceleration of the tank wall along its outward normal, $\ddot{x}_n$ equals to $\ddot{x}\cos\theta$. The load vector in Eq. (21) can be expressed as $\{F_{el}\} = -\int_{B_s} \rho_f N_i \ddot{x}_n \, \mathrm{d}s$.

3. Numerical examples, results and discussion

Example 1. The following three aspects analyzed by previous researchers are considered here to validate the present element formulation developed for the liquid, annular plate (baffle) and circular cylindrical tank.

Table 1
Slosh frequencies of liquid, ω_{nm}(rad/s) in a cylindrical rigid tank for different circumferential wave number, n and radial wave number, m ($R = 25.0$ m, $H = 21.6$ m)

m	Present study			
	$n = 1$	$n = 2$	$n = 3$	$n = 4$
1	0.81563 (0.81540)[a]	1.08973	1.28413	1.44619 (1.4444)[b]
2	1. 44925 (1.44624)[a]	1.62680	1.78007	1.91746 (1.9085)[b]
3	1.84073 (1.83020)[a]	1.99181	2.12779	2.25286 (2.2308)[b]
4	2.16739 (2.14323)[a]	2.30307	2.42823	2.54534 (2.5029)[b]
5	2.46020 (2.41362)[a]	2.58598	2.70398	2.81578 (2.7445)[b]

[a] Aslam et al. [7].
[b] Amabili et al. [26].

(i) The slosh frequencies of liquid in a cylindrical rigid tank of radius R and liquid depth H are computed for different circumferential wave number, n and radial wave number, m. The number of fluid elements are 200. It is observed from Table 1 that the slosh frequencies of liquid increase with the increase in either circumferential wave number or radial wave number or both. The present results are in good agreement with the slosh frequencies obtained from analytical expression given by Aslam et al. [7] for $n = 1$ and those of Amabili et al. [26] for $n = 4$ and different values of m. The sloshing mode shapes for the liquid pressure at the tank wall and slosh response at the liquid free surface is shown in Fig. 3.

(ii) An annular plate is used as baffle in the present study. The baffle is fixed at the outer periphery and free at inner periphery. The number of baffle elements are 20, 18, 16 and 14 for $R_i/R = 0.1, 0.3, 0.5$ and 0.7, respectively.

The natural frequencies of a baffle expressed as non-dimensional parameters are evaluated for different ratios of outer and inner radii. The geometrical and material properties are same as those of Amabili et al. [21]. The results presented in Table 2 for different circumferential wave number, n and radial wave number, m agree well with those of Amabili et al. [21].

(iii) A vertical circular cylindrical tank considered here is same as that of To and Wang [16]. The E, v and ρ are 210 GPa, 0.3 and 7800 kg/m^3, respectively. The number of shell elements are 20. The natural frequencies are computed for different circumferential wave number, n and longitudinal wave number, l. The results presented in Fig. 4 compare well with To and Wang [16].

Example 2. A cylindrical steel tank partially filled with water is considered for the coupled vibration frequency analysis with and without considering the free-surface waves. The geometrical and material properties are as follows:

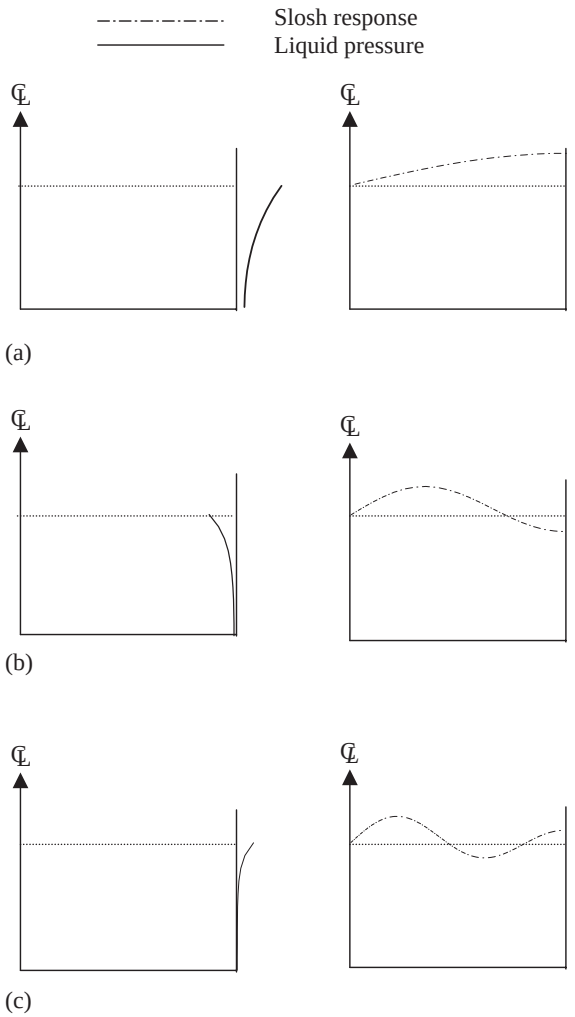

Fig. 3. Sloshing mode shapes corresponding to circumferential wave number, $n = 1$. (a) Mode 1 ($\omega_{11} = 0.81563$ rad/s); (b) Mode 2 ($\omega_{12} = 1.44925$ rad/s); (c) Mode 3 ($\omega_{13} = 1.84073$ rad/s).

Tank: radius (R) = 12.2 m; height (H_T) = 12.2 m; $E = 207$ GPa; $v = 0.3$; $\rho = 7830$ kg/m^3.
Liquid: depth of water (H) = 6.1 m; mass density of water (ρ_f) = 1000 kg/m^3.
Filling ratio: $H/H_T = 0.5$.
Number of fluid and shell elements are 200 and 20, respectively.

The slosh frequencies of liquid in a flexible tank are computed for the different tank wall thicknesses and are listed in Table 3. The percentage variations of slosh frequencies with respect to those for a rigid-tank sloshing model are presented in brackets. The higher variation of slosh frequencies are observed in lower modes. The variations are reported to be higher for lower thickness of the tank wall, which reflects the effect of flexibility of the tank on the slosh frequencies of liquid.

Table 2
Natural frequency parameters, $\bar{\omega}_{nm} = [\omega^2_{nm}\rho t R^4/D]^{1/4}$ of an annular plate for different circumferential wave number, n and radial wave number, m

n	m	Source	R_i/R			
			0.1	0.3	0.5	0.7
1	1	A	4.60376	4.42044	4.69197	6.73293
		B	4.60476	4.42044	4.69197	6.73293
1	2	A	7.75000	7.73044	9.86795	15.92875
		B	7.74991	7.73042	9.86794	15.92870
1	3	A	10.82091	11.77556	15.97060	26.34045
		B	10.82050	11.77540	15.97040	26.33990
1	4	A	13.87893	16.07834	22.17196	36.76523
		B	13.87790	16.07760	22.17100	36.76250
2	1	A	5.87668	5.70911	5.66705	7.18228
		B	5.87668	5.70911	5.66706	7.18228
2	2	A	9.13667	8.89166	10.36756	16.12189
		B	9.13664	8.89161	10.36760	16.12180
2	3	A	12.30226	12.50895	16.23468	26.44154
		B	12.30210	12.50870	16.23450	26.44100
2	4	A	15.42929	16.56367	22.34706	36.83367
		B	15.42840	16.56290	22.34600	36.83090
3	1	A	7.14070	7.00493	6.76847	7.82877
		B	7.14069	7.00493	6.76847	7.82877
3	2	A	10.52531	10.20124	11.09287	16.43301
		B	10.52520	10.20120	11.09290	16.43300
3	3	A	13.76565	13.54141	16.65726	26.60860
		B	13.76530	13.54110	16.65710	26.60800
3	4	A	16.94544	17.31420	22.63375	36.94732
		B	16.94450	17.31320	22.63270	36.94460

A: Present study; B: Amabili et al. [21].

The slosh frequencies and coupled vibration frequencies are calculated for the above liquid–tank system and are presented in Table 4. Here the tank wall thickness is taken as 12.2 mm. The results presented in Table 4 compare well with those given by Balendra et al. [9]. This comparison validates the present coupled formulation for the liquid–flexible tank system. The coupled vibration frequencies without considering sloshing of liquid are also presented in Table 4 and are found to be lower than the coupled frequencies by taking sloshing into account. This is because of the assumption of zero dynamic pressure on the undisturbed liquid free surface, which overestimates the hydrodynamic mass of the system.

Example 3. A partially filled cylindrical flexible tank with a flexible baffle is considered. The depth, H of the liquid is considered same as the radius, R of the tank. A baffle is placed at a depth h from the liquid free surface and h' from the top of the tank. The dimension and material properties of tank and baffle are presented below.

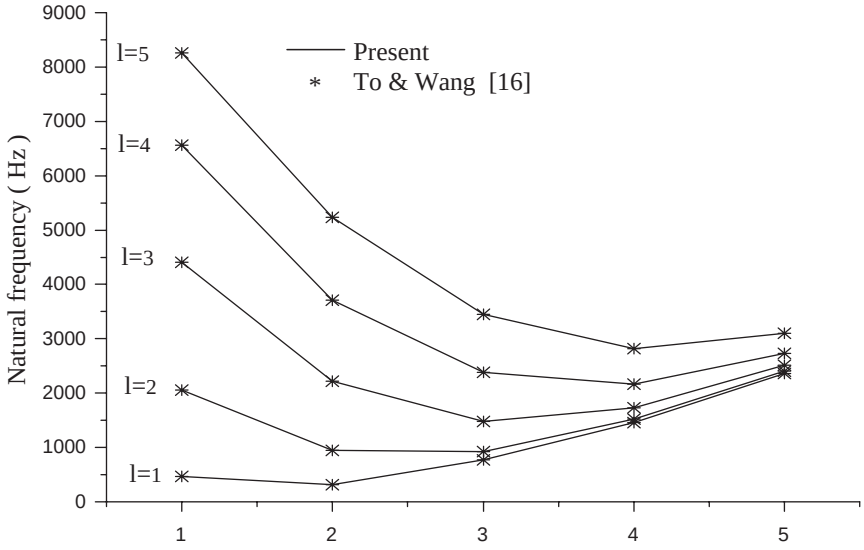

Fig. 4. Natural frequencies of a cylindrical steel tank with various circumferential number, n and longitudinal number, l (radius = 63.5 mm, height = 502 mm and thickness = 1.63 mm).

Table 3
Slosh frequencies ω_{lm}(Hz) with respect to tank wall thickness for different radial wave number, m and circumferential wave number as one

m	Rigid-tank sloshing model	Flexible-tank sloshing model				
		Thickness of tank (mm)				
		0.5	1.0	5.0	10.0	100
1	0.16516	0.16388 (0.775%)	0.16452 (0.387%)	0.16504 (0.072%)	0.16510 (0.072%)	0.16516 (0%)
2	0.32989	0.32929 (0.181%)	0.32959 (0.090%)	0.32983 (0.018%)	0.32986 (0.009%)	0.32989 (0%)
3	0.42373	0.42326 (0.110%)	0.42350 (0.054%)	0.42368 (0.011%)	0.42368 (0.002%)	0.42373 (0%)
4	0.50424	0.50382 (0.042%)	0.50403 (0.021%)	0.50420 (0.004%)	0.50422 (0.002%)	0.50424 (0%)

Note: The bracketed values are the variation of frequencies compared to rigid-tank sloshing model.

Tank: $R = 508$ mm; $H_T = 520.7$ mm; $t_t = 1.0$ mm; $H = 508$ mm.
Filling ratio: $H/H_T = 0.975$.
Baffle: $R_i = 304.8$ mm; $R = 508$ mm; $t_b = 1.0$ mm.
Material properties (tank and baffle): $E = 103$ GPa; $v = 0.3$; $\rho_s = 4500$ kg/m^3.

Number of fluid elements are 184, 188, 190 and 192 for $R_i/R = 0.2$, 0.4, 0.6 and 0.8, respectively. Number of shell elements are 13. Number of baffle elements are 16, 12, 10 and 8 for $R_i/R = 0.2$, 0.4, 0.6 and 0.8, respectively.

Table 4
Natural frequencies (Hz) of the coupled system ($n = 1$)

Type of frequencies	Mode number	Balendra et al. [9] (Sloshing considered)	Present study	
			Sloshing considered	Sloshing neglected
Sloshing frequencies	1	0.16470	0.16511	—
	2	0.32893	0.32987	—
	3	0.42229	0.42371	—
	4	0.50218	0.50422	—
	5	0.57745	0.58024	—
	6	0.65154	0.65513	—
	7	0.72522	0.72966	—
	8	0.79563	0.80132	—
	9	0.85386	0.86210	—
	10	0.88456	0.89636	—
Coupled vibration frequencies	11	9.64375	9.63578	9.63288
	12	17.61110	17.63045	17.62894
	13	24.00300	24.15363	24.15251
	14	29.59760	29.96432	29.96327
	15	35.60210	36.31080	36.30977

The free vibration characteristics of tank–baffle system are studied under both empty and liquid-filled conditions.

3.1. Empty tank–baffle system

The tank–baffle system is assumed to be clamped at the tank base and free at the top. First, the natural frequencies of tank without baffle are computed and are presented in Table 5. Then the natural frequencies of the tank with baffle are computed for different h'/H_T ratios and $R_i/R = 0.6$ and are recorded in Table 5, where the superscripts 'B' and 'T' indicate the baffle and tank-wall dominated mode frequencies, respectively. It is observed from results in Table 5 that the five lowest frequencies are baffle-dominated mode frequencies and others are tank-dominated mode frequencies for all h'/H_T ratios. The tank-dominated mode frequencies are observed to be higher than the frequencies of tank without baffle.

The natural frequencies of tank–baffle system are computed for different R_i/R ratios and $h'/H_T = 0.12$ and are presented in Table 6. The fundamental mode frequencies are baffle-dominated modes for all R_i/R ratios. The tank-dominated mode frequencies are independent of R_i/R ratios, whereas the baffle-dominated mode frequencies vary as shown in Table 6.

The longitudinal mode shape of the first four lowest frequencies of the tank without baffle are illustrated in Fig. 5. The mode shape for first eight lowest frequencies of the tank with baffle are illustrated in Fig. 6 for the baffle position, $h'/H_T = 0.12$ and $R_i/R = 0.6$. It is observed from Fig. 6 that the longitudinal mode shapes of the tank are changed in presence of baffle, and the radial displacements of the tank are restrained at the baffle location.

Table 5
Natural frequencies (Hz) of an empty tank–baffle system for different h'/H_T ratios and $R_i/R = 0.6$ ($n = 1$)

Mode number	Tank	Tank–baffle system h'/H_T ratios			
		0.22	0.32	0.41	0.51
1	851.32	25.66^{B}	25.66^{B}	25.66^{B}	25.66^{B}
2	1426.38	130.64^{B}	130.64^{B}	130.64^{B}	130.64^{B}
3	1475.42	351.51^{B}	351.51^{B}	351.51^{B}	351.51^{B}
4	1498.38	682.99^{B}	682.99^{B}	682.99^{B}	682.99^{B}
5	1513.99	1128.38^{B}	1128.38^{B}	1128.38^{B}	1128.38^{B}
6	1534.54	1357.24^{T}	1341.65^{T}	1276.45^{T}	1194.05^{T}
7	1563.08	1450.20^{T}	1426.70^{T}	1436.66^{T}	1454.40^{T}
8	1604.50	1479.45^{T}	1489.42^{T}	1497.59^{T}	1485.76^{T}
9	1664.49	1507.15^{T}	1514.73^{T}	1501.90^{T}	1517.26^{T}
10	1734.29	1536.92^{T}	1520.11^{T}	1540.31^{T}	1520.55^{T}

The values with superscripts 'B' and'T' indicate baffle and tank-wall dominated mode frequencies.

Table 6
Natural frequencies (Hz) of an empty tank–baffle system for different R_i/R ratios and $h'/H_T = 0.12$ ($n = 1$)

Mode number	R_i/R ratios			
	0.2	0.4	0.6	0.8
1	18.34^{B}	17.49^{B}	25.66^{B}	84.48^{B}
2	50.80^{B}	64.48^{B}	130.64^{B}	501.93^{B}
3	104.54^{B}	161.63^{B}	351.51^{B}	1336.52^{T}
4	185.36^{B}	308.11^{B}	682.99^{B}	1396.55^{B}
5	394.39^{B}	504.14^{B}	1128.38^{B}	1468.61^{T}
6	431.53^{B}	750.13^{B}	1336.52^{T}	1495.52^{T}
7	596.82^{B}	1047.02^{B}	1468.61^{T}	1502.91^{T}
8	790.48^{B}	1336.52^{T}	1495.52^{T}	1521.55^{T}
9	1012.94^{B}	1396.30^{B}	1502.91^{T}	1880.69^{T}
10	1264.83^{B}	1468.61^{T}	1521.55^{T}	1968.80^{T}
11	1336.52^{T}	1495.52^{T}	1550.65^{T}	2110.90^{T}
12	1468.61^{T}	1502.91^{T}	1596.36^{T}	2365.10^{T}

The values with superscripts 'B' and 'T' indicate baffle and tank-wall dominated mode frequencies.

3.2. Liquid-filled tank–baffle system

The coupled formulation developed for the flexible-tank–flexible-baffle system is applied to a liquid-filled rigid-tank with rigid-baffle system. For the case, E is assumed to be 10^{20} GPa. The slosh frequency parameters ($\bar{\omega}_{lm} = \omega_{lm}(R/g)^{1/2}$) are computed for different R_i/R ratios and for two different radial modes ($m = 1$ and 2) and its squared values are presented in Fig. 7 for comparison. It is observed that the computed results are quite comparable with those of Gedikli and Ergüven [27].

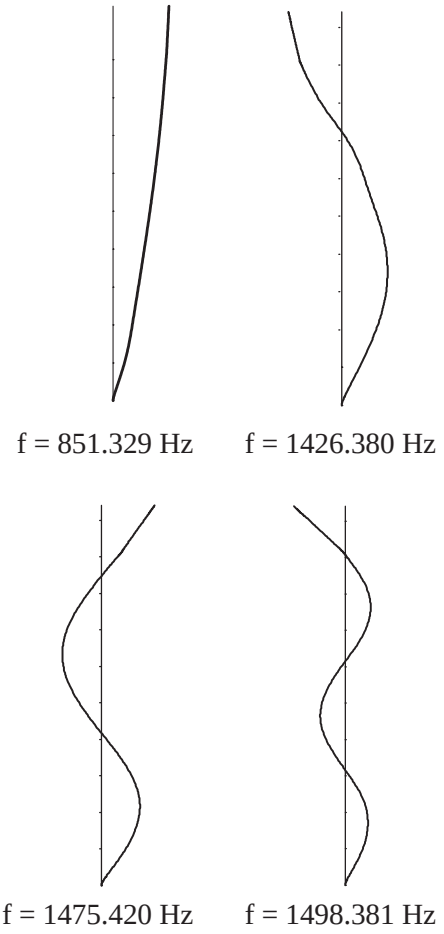

Fig. 5. Longitudinal mode shapes of four lowest natural frequencies of an empty tank corresponding to circumferential wave number, $n = 1$.

The fundamental slosh frequency of liquid in the flexible tank without baffle is determined as 0.925 Hz and is illustrated in Fig. 8 as a straight line (curve no. 1). The fundamental slosh frequencies of liquid are computed for different positions of the flexible baffle, i.e., $h/H = 0.1$–0.8 and $R_i/R = 0.6$ and are presented in Fig. 8 (curve no. 2). It is observed that the baffle placed near to the free surface has a greater influence on the slosh frequencies. The effect of baffle is gradually reduced when it is moved towards the bottom of the tank. The slosh frequencies of liquid are also computed by varying the dimension of the baffle i.e., $R_i/R = 0.2$–0.8 and $h/H = 0.1$. The results are presented in Fig. 9 (curve no. 2). It is seen that the slosh frequencies of liquid decrease with the decrease of R_i/R ratios.

The slosh frequencies of liquid are also computed for a rigid-tank–rigid-baffle system. Curve no. 3 in Figs. 8 and 9 represent the variations of slosh frequencies for rigid-tank–rigid-baffle system for different $h/H$and R_i/R ratios. It is observed from Figs. 8 and 9 that the flexibility of tank–baffle system has a little effect on the slosh frequencies.

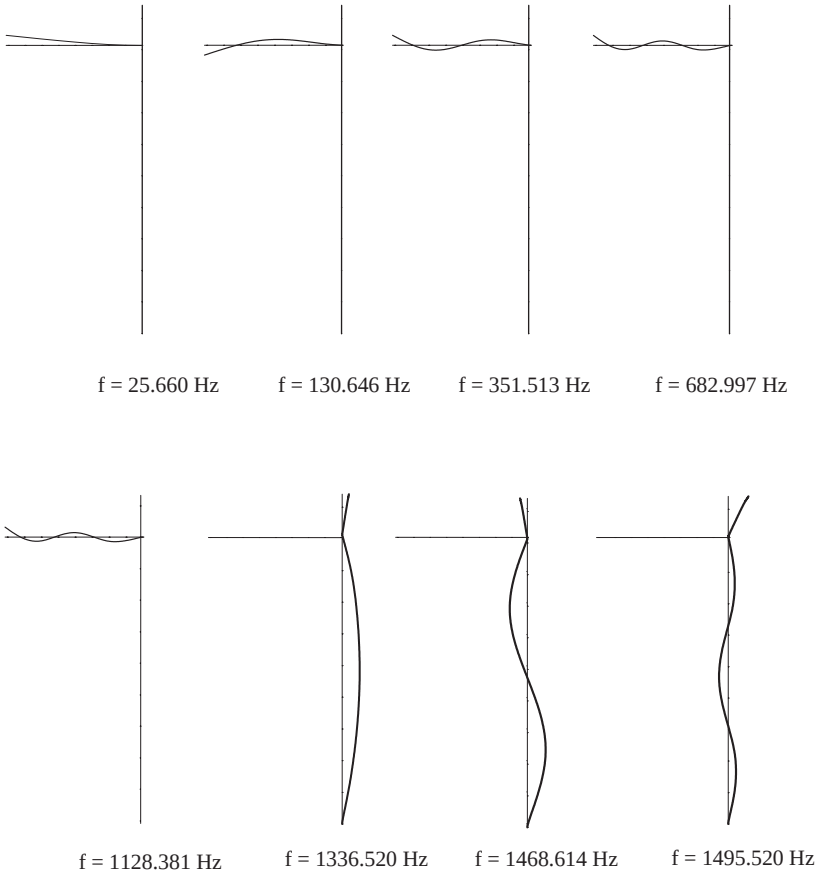

Fig. 6. Mode shapes of eight lowest natural frequencies of an empty tank–baffle system corresponding to circumferential wave number, $n = 1$.

The coupled frequencies of tank without baffle are computed considering the effect of sloshing of liquid and are presented in Table 7. The coupled frequencies of the tank with baffle are computed for different h/H ratios and $R_i/R = 0.6$ and are recorded in Table 7, where the superscripts 'B' and 'M' indicate the baffle-dominated and mix mode frequencies, respectively. The first four lowest coupled frequencies and their corresponding mode shapes are shown in Fig. 10 for the liquid–tank system without baffle. Fig. 11 illustrates the mode shapes of the first eight lowest coupled frequencies of the liquid–tank–baffle system for the baffle position, $h/H = 0.1$ and $R_i/R = 0.6$.

It is observed from Table 7 that the fundamental modes are for baffle-dominated modes for all positions of the baffle in a tank. The baffle-dominated mode frequencies decrease with the increase in (h/H) ratios. This happens as the dynamic mass of the liquid increases as the baffle is placed towards the bottom of the tank.

Example 4. The sloshing response of liquid in a cylindrical rigid tank without baffle is studied under sinusoidal horizontal base acceleration, $\ddot{x} = -x_0\omega^2 \sin \omega t$. The radius (R) of the tank is

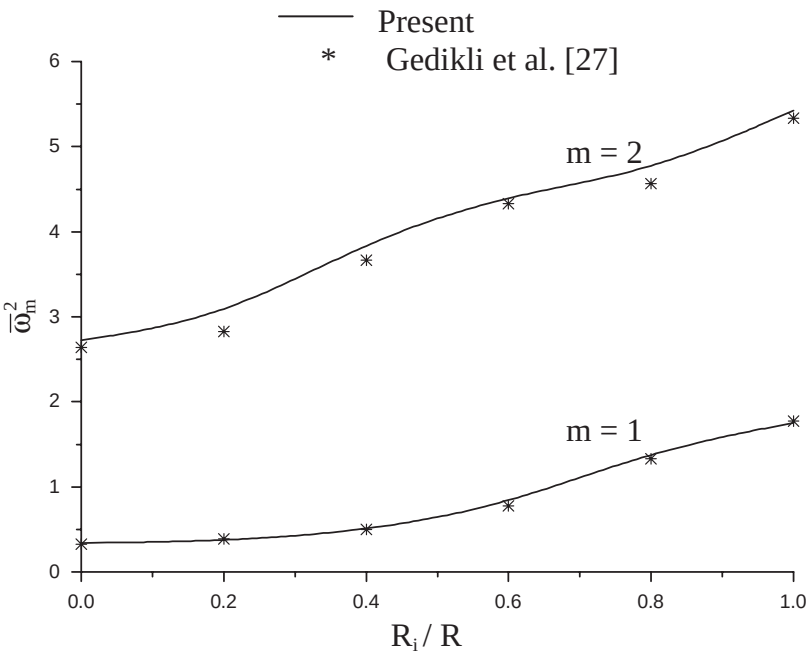

Fig. 7. Variation of natural frequencies of liquid with R_i/R ($H/R = 1.0$ and $h/H = 0.1$).

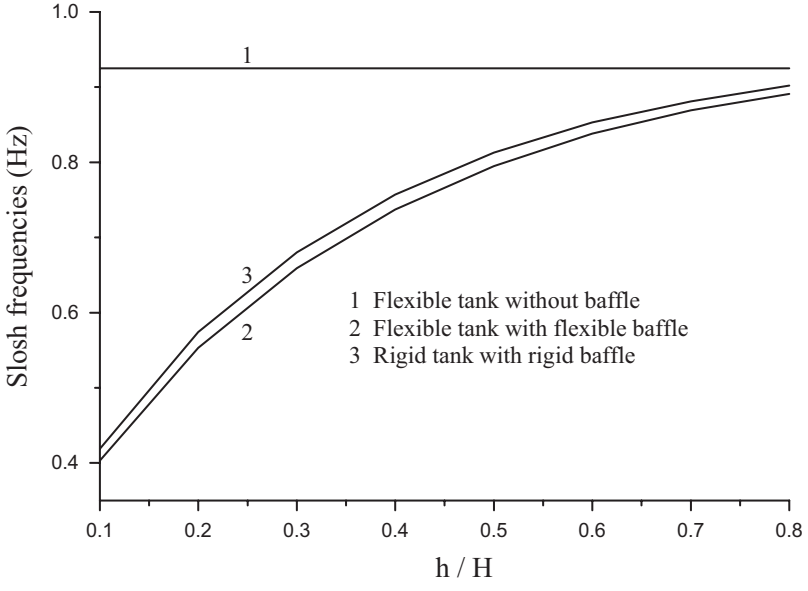

Fig. 8. Slosh frequencies of liquid for different h/H ratios ($H/R = 1.0$ and $R_i/R = 0.2$).

0.508 m and liquid depth (H) in the tank is 0.508 m. The density of the liquid (ρ_f) is 1000.0 kg/m^3. The parameter x_0 is taken as 0.001 m and the exciting frequencies ω are 5.811, 10.235, 13.169 and 15.814 rad/s which correspond to first four lowest frequencies of liquid. The number of fluid

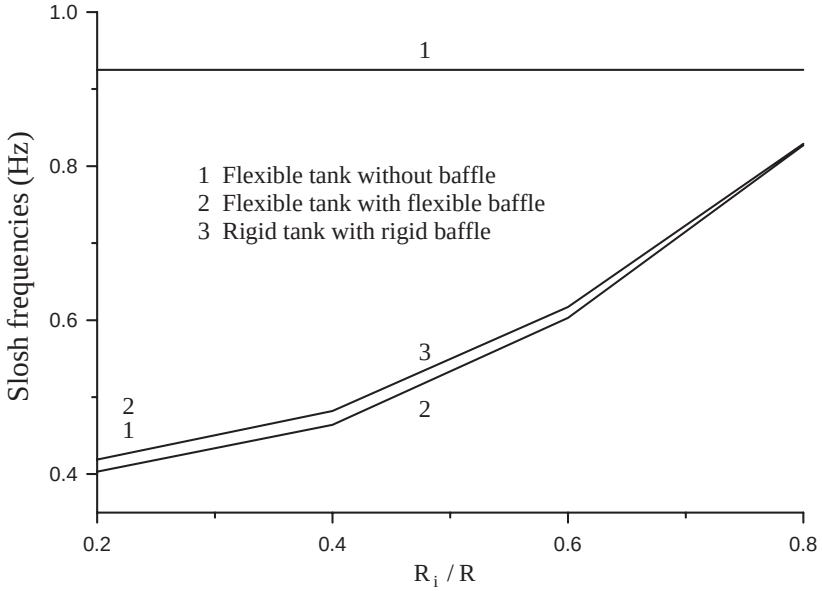

Fig. 9. Slosh frequencies of liquid for different R_i/R ratios ($H/R = 1.0$ and $h/H = 0.1$).

Table 7
Coupled frequencies (Hz) of a partially filled tank with and without baffle ($n = 1$)

Mode number	Tank	Tank–baffle system h/H ratios				
		0.1	0.2	0.3	0.4	0.5
1	143.457	4.611^{B}	4.019^{B}	3.705^{B}	3.486^{B}	3.307^{B}
2	277.582	30.423^{B}	29.004^{B}	28.486^{B}	28.254^{B}	28.128^{B}
3	396.236	102.929^{B}	100.939^{B}	100.552^{B}	100.429^{B}	100.429^{B}
4	493.066	169.245^{M}	174.588^{M}	181.626^{M}	190.005^{M}	198.617^{M}
5	592.011	248.735^{B}	248.344^{B}	248.386^{B}	247.362^{B}	243.679^{B}
6	698.978	298.869^{M}	307.968^{M}	314.548^{M}	300.743^{M}	281.232^{M}
7	813.609	395.426^{M}	410.556^{M}	381.426^{M}	376.649^{M}	399.475^{M}
8	979.022	477.413^{M}	463.017^{M}	457.548^{M}	488.604^{M}	452.915^{M}
9	1344.270	517.256^{M}	503.631^{M}	514.123^{M}	494.449^{M}	517.717^{M}
10	1473.071	579.963^{M}	562.280^{M}	580.393^{M}	565.319^{M}	584.418^{M}

The values with superscripts 'B' and 'M' indicate baffle-dominated and mixed-mode frequencies.

elements are 200. The slosh displacement at the wall are computed over a period of 10 s and presented in Fig. 12. It is observed that the sloshing amplitude is the largest when the first sloshing mode is used as the exciting frequencies.

The sloshing response of liquid in a cylindrical rigid tank in presence of rigid baffle is studied under the same loading condition. The parameters x_0 and ω are taken to be as 0.001 m and 5.811 rad/s, respectively. The thickness of baffle is 0.001 m and is assumed to be rigid. The effect of baffle on the slosh response is studied by varying the dimension and position of the baffle. The

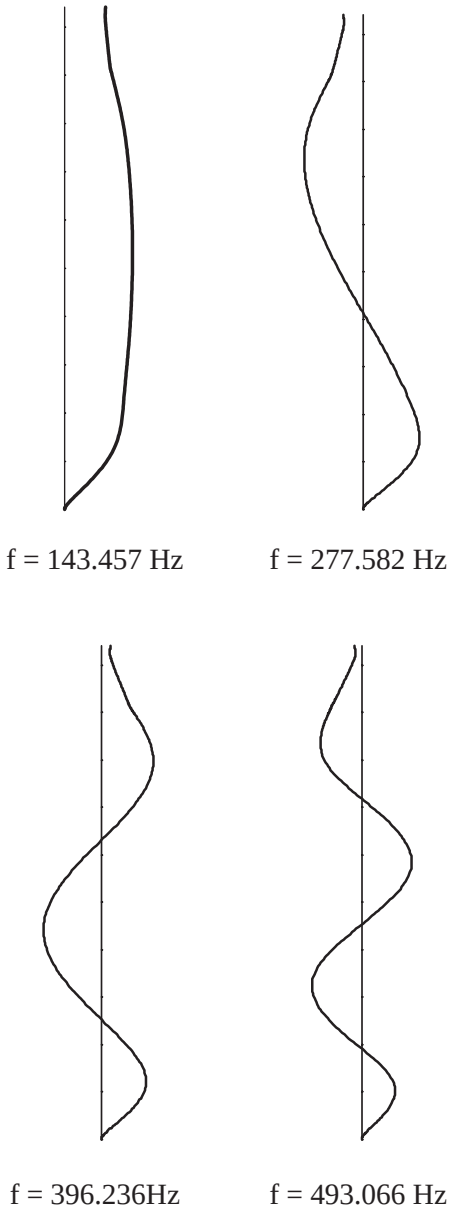

Fig. 10. Longitudinal mode shapes of four lowest coupled frequencies of partially filled tank corresponding to circumferential wave number, $n = 1$.

slosh displacement at the tank wall are computed for $h/H = 0.1$ and R_i/R ratios are equal to 0.8, 0.6 and 0.4 and are presented in Fig. 13. The slosh displacement at the tank wall are computed for $R_i/R = 0.6$ and h/H ratios are equal to 0.3 and 0.8 and are illustrated in Fig. 13. The maximum slosh amplitude obtained from Figs. 13 and 14 are tabulated in Table 8, and the percentage of reduction in slosh amplitude compared to tank without baffle are presented within brackets. It is

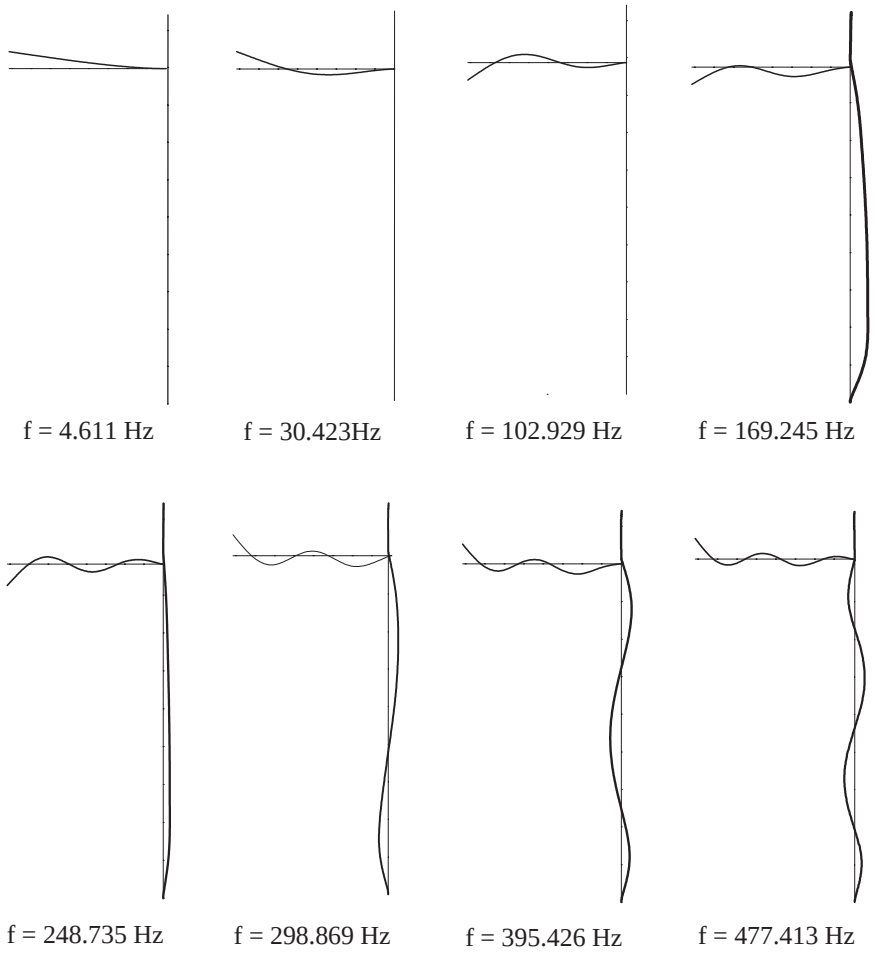

Fig. 11. Modes for eight lowest coupled frequencies of a partially filled tank–baffle system corresponding to circumferential wave number, $n = 1$.

Table 8
Maximum slosh displacements (m) at the tank wall in a partially filled tank with a baffle of varying dimension and located at different depth (h) from liquid free surface

h/H	R_i/R		
	0.4	0.6	0.8
0.1	0.0016	0.0036	0.0166
	(96.12%)	(91.28%)	(59.80%)
0.3	0.0051	0.0100	0.0344
	(87.76%)	(75.78%)	(16.70%)
0.8	0.0390	0.0406	0.0411
	(5.56%)	(1.69%)	(0.48%)

Note: The maximum slosh displacement (m) at tank wall without baffle is 0.0413.

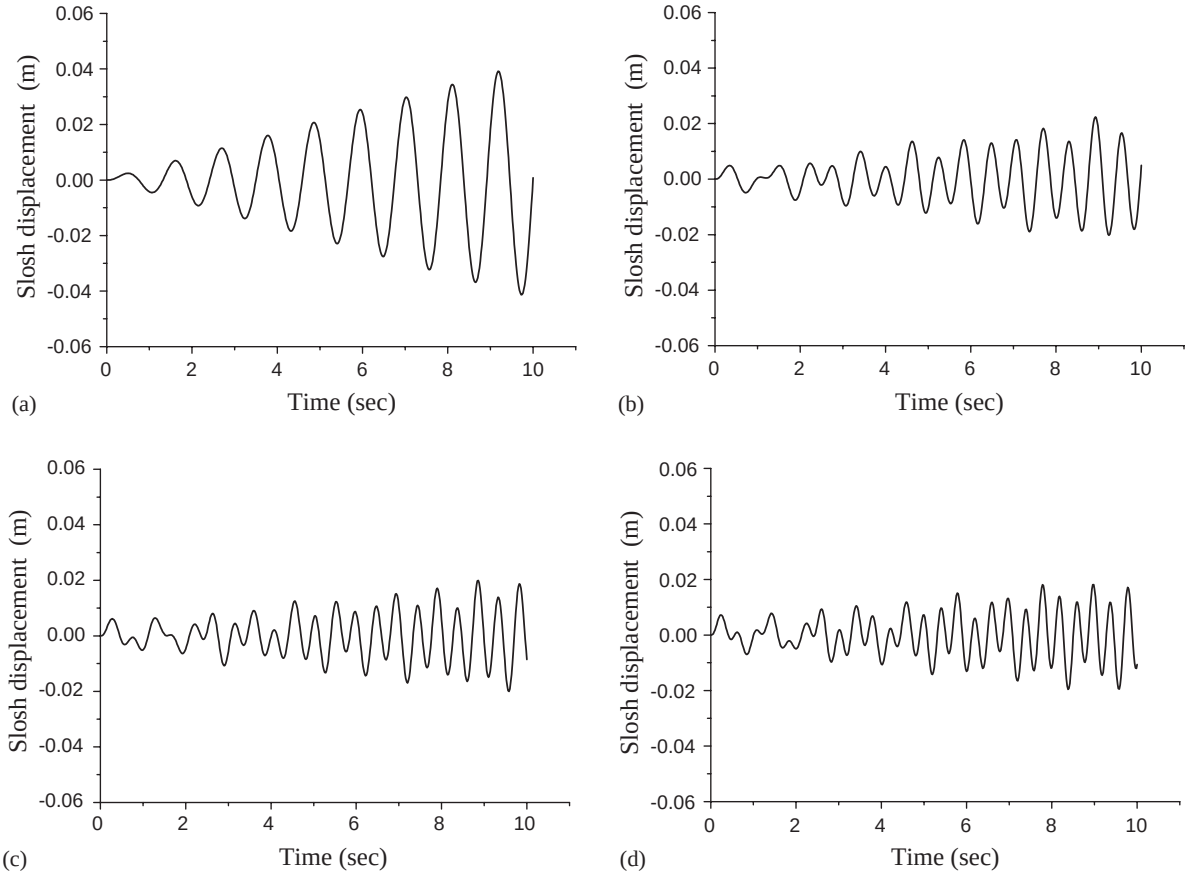

Fig. 12. Slosh displacements at tank wall in a cylindrical rigid tank under sinusoidal base excitation ($\ddot{x} = -0.001\omega^2 \sin \omega t$) using first four lowest slosh frequencies as exciting frequency. (a) $\omega = 5.811$ rad/s (1st mode); (b) $\omega = 10.235$ rad/s (2nd mode); (c) $\omega = 13.169$ rad/s (3rd mode); (d) $\omega = 15.814$ rad/s (4th mode).

observed from Table 8 that the slosh amplitude decreases with the decrease in R_i/R ratios and increases with the increase in h/H ratios. The maximum reduction (96.12%) of slosh displacement at the tank wall is observed when the baffle is placed at $h/H = 0.1$ for $R_i/R = 0.4$. The baffle placed very close to the tank bottom does have negligible contribution in damping out the slosh amplitude of liquid.

Example 5. A flexible cylindrical tank with a flexible baffle is considered here to study the flexibility of tank–baffle system on the slosh amplitude of liquid. It is subjected to sinusoidal horizontal base acceleration, $\ddot{x} = -x_0\omega^2 \sin \omega t$. The parameters x_0 and ω are taken to be as 0.001 m and 5.811 rad/s, respectively. The radius of the tank, R and the liquid depth, H are the same as that of Example 4 and height of the tank is 0.525 m. The filling ratio, H/H_T is 0.968. The thickness of baffle is taken to be as 0.001 m and the same thickness is used for the tank wall. The E

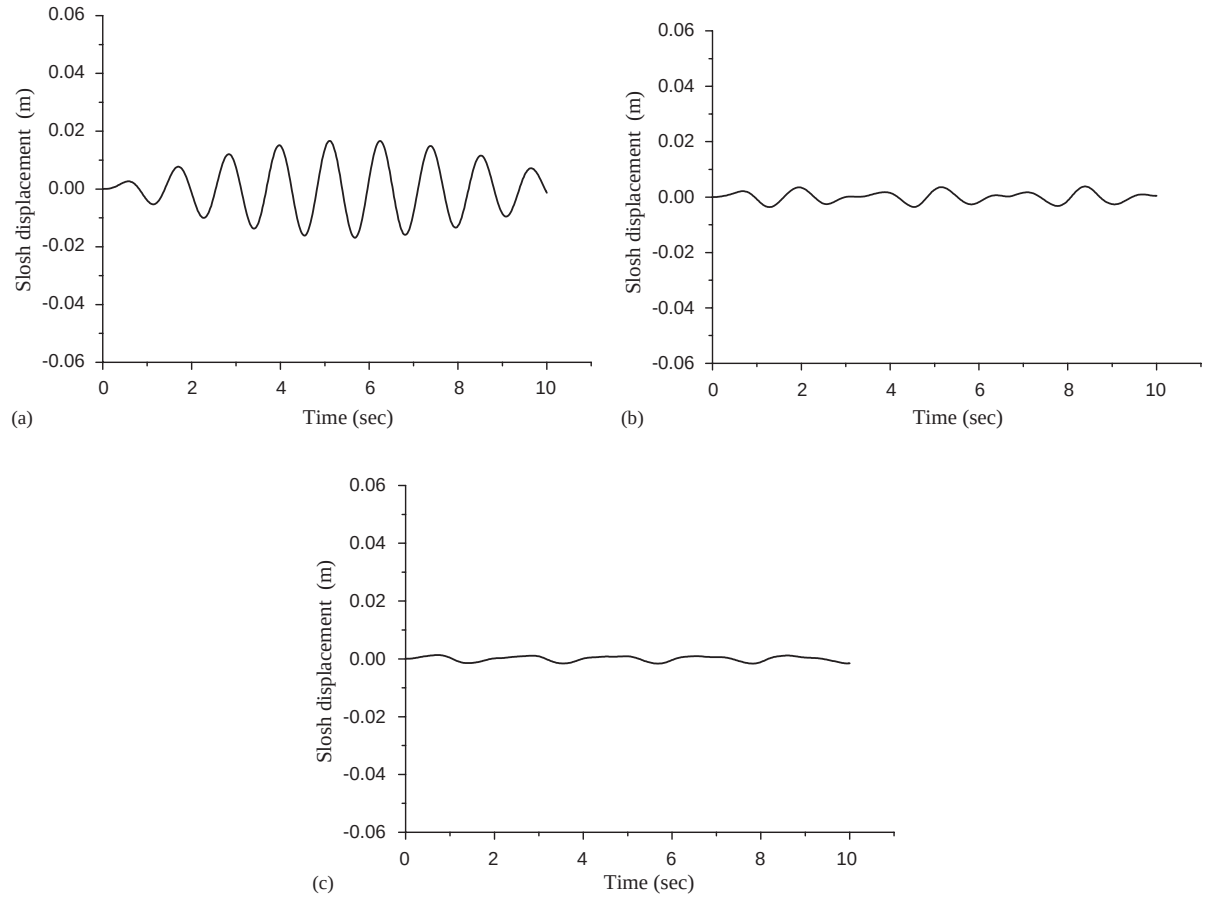

Fig. 13. Slosh displacements at tank wall in a cylindrical rigid tank with varying R_i/R ratios of baffle under sinusoidal base excitation, $\ddot{x} = -x_0\omega^2 \sin \omega t$ ($x_0 = 0.001$ m, $\omega = 5.811$ rad/s. (a) Tank with baffle ($R_i/R = 0.8$, $h/H = 0.1$); (b) tank with baffle ($R_i/R = 0.6$, $h/H = 0.1$); (c) tank with baffle ($R_i/R = 0.4$, $h/H = 0.1$).

and ρ of the tank and baffle materials are taken to be as 103 GPa and 4500 kg/m^3, respectively. The number of fluid, baffle and shell elements are 192, 10 and 13, respectively. The slosh displacement at the wall are computed over a period of 10 s and are presented in Fig. 15. The slosh displacement of liquid at the tank wall are computed for the rigid-tank–flexible-baffle and rigid-tank–rigid-baffle systems and are also presented in Fig. 15. It is observed that the flexibility of a baffle has a significant effect on the slosh response of the liquid, whereas the flexibility of the tank has little effect.

4. Conclusion

A coupled finite element formulation is developed to compute the natural frequencies of liquid and liquid-filled tank–baffle system. The slosh frequencies of a non-viscous and incompressible

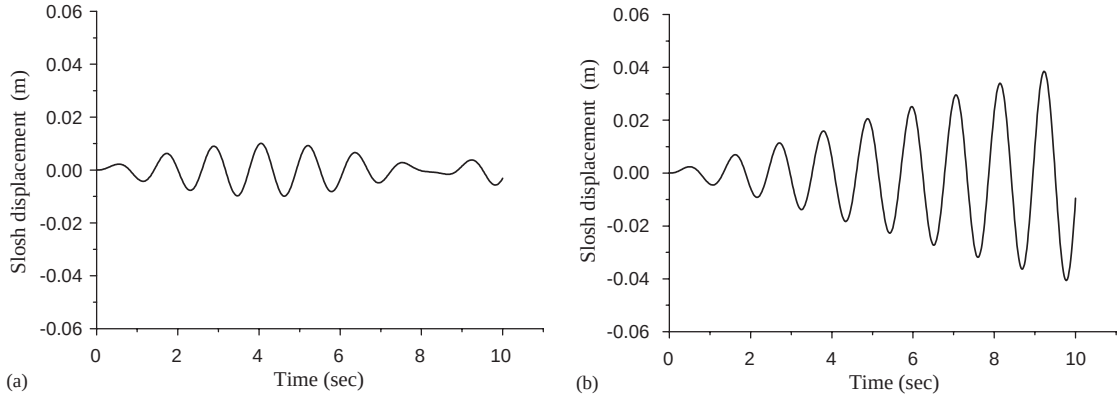

Fig. 14. Slosh displacements at tank wall in a cylindrical rigid tank with varying h/H ratios of baffle under sinusoidal base excitation, $\ddot{x} = -x_0\omega^2 \sin \omega t$ ($x_0 = 0.001$ m, $\omega = 5.811$ rad/s). (a) Tank with baffle ($R_i/R = 0.6$, $h/H = 0.3$); (b) tank with baffle ($R_i/R = 0.6$, $h/H = 0.8$).

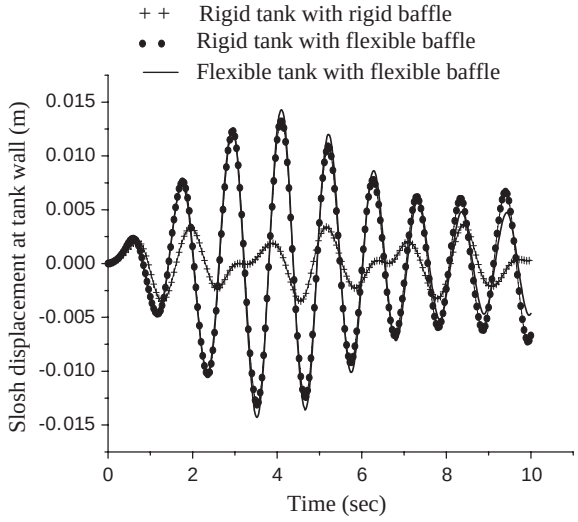

Fig. 15. Slosh displacements at tank wall in a cylindrical tank with baffle ($R_i/R = 0.6$ and $h/H = 0.1$) under sinusoidal base excitation, $\ddot{x} = -x_0\omega^2 \sin \omega t$ ($x_0 = 0.001$ m, $\omega = 5.811$ rad/s).

liquid are evaluated for different dimensions and positions of an annular circular baffle attached to the tank wall. The slosh frequencies of liquid in a tank can be reduced by the use of the baffle. The baffle has greater influence on the slosh frequencies of liquid when placed near to the liquid free surface and the influence is gradually reduced when it is moved towards the bottom of the tank. The effect of the flexibility of the tank–baffle system on the slosh frequencies of liquid is examined. It is reported that the slosh frequencies of liquid in the flexible-tank–baffle system are lower than those of the rigid system.

The slosh amplitude of liquid in a rigid tank is computed under a sinusoidal horizontal base excitation. The rigid baffle is placed at different locations in a liquid-filled cylindrical rigid tank

and its effect is examined. The slosh amplitude of liquid can be reduced to a maximum limit by placing the baffle close to free surface. The effects of flexibility of the tank wall and baffle on the slosh response of liquid are studied. The flexibility of both tank and baffle affects the slosh response of liquid, but the latter has a higher effect. The slosh amplitude of liquid in a tank with a flexible baffle is found to be higher than that in the case with a rigid baffle, but is lower than that without a baffle. Hence, an annular baffle can be successfully used in damping out the slosh amplitude of liquid in a cylindrical tank.

Appendix A. Nomenclature

R radius of tank
H depth of liquid in the tank
H_T height of the tank
E Young's modulus of tank and baffle material
v the Poisson ratio
ρ_f mass density of liquid
ρ_s mass density of tank and baffle material
t_t, t_b thickness of tank wall and baffle, respectively
R_1 inner radius of annular ring element of baffle
R_2 outer radius of annular ring element of baffle
h depth of baffle from liquid free surface
$[K_f]$ global stiffness matrix of the liquid
$[M_f]$ global mass matrix of the liquid
$[K_s]$ global stiffness matrix of the tank–baffle system
$[M_s]$ global mass matrix of the tank–baffle system
$[S]$ coupling matrix
B_f liquid free-surface boundary
B_s liquid–structure interface boundary
B_b tank bottom boundary

References

[1] G.W. Housner, Dynamic pressure on accelerated fluid containers, *Bulletin of Seismological Society of America* 47 (1) (1957) 15–35.
[2] G.W. Housner, The dynamic behaviour of water tanks, *Bulletin of Seismological Society of America* 53 (1963) 381–387.
[3] H.N. Abramson, The dynamic behaviour of liquids in moving containers, 1966 NASA SP-106, Washington, DC.
[4] O.C. Zienkiewicz, P. Bettess, Fluid–structure dynamic interaction and water forces. An introduction to numerical treatment, *International Journal for Numerical Methods in Engineering* 13 (1978) 1–16.
[5] M.A. Haroun, G.W. Housner, Earthquake response of deformable liquid storage tanks, *American Society of Mechanical Engineers, Journal of Applied Mechanics* 48 (1981) 411–418.
[6] M. Aslam, Finite element analysis of earthquake-induced sloshing in axisymmetric tanks, *International Journal for Numerical Methods in Engineering* 17 (1981) 159–170.

[7] M. Aslam, W.G. Godden, D.T. Scalise, Earthquake sloshing in annular and cylindrical tanks, *American Society of Civil Engineers, Journal of Engineering Mechanics* 105 (3) (1979) 371–389.
[8] T.F. Li, C.C. Lin, C.H. Luk, Three-directional fluid pool seismic sloshing analysis, *American Society of Mechanical Engineers, Journal of Pressure Vessel Technology* 103 (1981) 10–15.
[9] T. Balendra, K.K. Ang, P. Paramasivam, S.L. Lee, Free vibration analysis of cylindrical liquid storage tanks, *International Journal of Mechanical Science* 24 (1) (1982) 47–59.
[10] D.C. Ma, J. Gvildys, Y.W. Chang, Seismic behaviour of liquid-filled shells, *Nuclear Engineering and Design* 70 (1982) 437–455.
[11] W.K. Liu, D.C. Ma, Coupling effect between liquid sloshing and flexible fluid-filled systems, *Nuclear Engineering and Design* 72 (1982) 345–357.
[12] L.G. Olson, K.J. Bathe, A study of displacement-based fluid finite elements for frequencies of fluid and fluid–structure system, *Nuclear Engineering and Design* 76 (1983) 137–151.
[13] E.L. Wilson, M. Khalvati, Finite elements for the dynamic analysis of fluid–solid systems, *International Journal of Numerical Methods in Engineering* 19 (1983) 1657–1668.
[14] R.K. Gupta, G.L. Hutchinson, Solid–water interaction in liquid storage tanks, *Journal of Sound and Vibration* 135 (3) (1989) 357–374.
[15] A. Pui-Chen Lui, Dynamic coupling of a liquid–tank system under transient excitations, *Journal of Ocean Engineering* 17 (3) (1990) 263–277.
[16] C.W.S. To, B. Wang, An axisymmetric thin shell finite element for vibration analysis, *Computers and Structures* 40 (3) (1991) 555–568.
[17] E. Kock, L. Olson, Fluid–structure interaction analysis by the finite element method—a variational approach, *International Journal for Numerical Methods in Engineering* 31 (1991) 463–491.
[18] A.A. Lakis, M. Sinno, Free vibration of axisymmetric and beam-like cylindrical shells, partially filled with liquid, *International Journal for Numerical Methods in Engineering* 33 (1992) 235–268.
[19] Wang Qinque, Huand Lidu, Eigen-problem of liquid–container coupling, *Computers and Structures* 44 (1/2) (1992) 353–355.
[20] H.F. Bauer, Coupled frequencies of a liquid in a circular cylindrical container with elastic liquid surface cover, *Journal of Sound and Vibration* 180 (1995) 689–704.
[21] M. Amabili, G. Frosali, M.K. Kwak, Free vibrations of annular plates coupled with fluids, *Journal of Sound and Vibration* 191 (5) (1996) 825–846.
[22] S.S. Babu, S.K. Bhattacharyya, Finite element analysis of fluid structure interaction effect on liquid retaining structures due to sloshing, *Computers and Structures* 59 (6) (1996) 1165–1171.
[23] P.B. Goncalves, N.R.S.S. Ramos, Free vibration analysis of cylindrical tanks partially filled with liquid, *Journal of Sound and Vibration* 195 (1996) 429–444.
[24] J.K. Kim, H.M. Koh, I.J.K. Wahk, Dynamic response of rectangular flexible fluid containers, *American Society of Civil Engineers, Journal of Engineering Mechanics* 122 (1996) 807–817.
[25] A. Bermudez, R. Duran, R. Rodriguez, Finite element solution of incompressible fluid–structure vibration problems, *International Journal for Numerical Methods in Engineering* 40 (1997) 1435–1448.
[26] M. Amabili, M.P. Paidoussis, A.A. Lakis, Vibrations of partially filled cylindrical tanks with ring-stiffeners and flexible bottom, *Journal of Sound and Vibration* 213 (2) (1998) 259–299.
[27] A. Gedikli, M.E. Ergüven, Seismic analysis of a liquid storage tank with a baffle, *Journal of Sound and Vibration* 223 (1) (1999) 141–155.
[28] J.R. Cho, J.M. Song, Assessment of classical numerical models for the separate fluid–structure modal analysis, *Journal of Sound and Vibration* 239 (5) (2001) 995–1012.
[29] K.C. Biswal, S.K. Bhattacharyya, P.K. Sinha, Free vibration analysis of liquid filled tank with baffles, *Journal of Sound and Vibration* 259 (1) (2003) 177–192.
[30] V.V. Novozhilov, *Thin Shell Theory*, P. Noordhoff Ltd, Groningen, The Netherlands, 1964.